Chapter 4

Plasma Nitriding of Medium Carbon Low Alloy Steels

4.1 Introduction

The classification of steels is generally made on the basis of carbon percentage mixed with iron. Steels which have the carbon percentage ~0.25 wt% to 0.6 wt% were categorized as medium carbon steel. These steels are generally used after heat treatment (quenching and tempering) for various applications such as, railway wheels, tracks, gears and crankshaft etc. Further the addition of other alloying elements such as Chromium (Cr), Molybdenum (Mo), Tungsten (W), Vanadium (V), Aluminum (Al) and Nickel (Ni) increase its mechanical properties (strength, wear resistance and hardness). On the basis of these extra added alloying elements, steels are further classified such as; medium carbon low alloy steels and medium carbon high alloy steels. If the total amount of extra added alloying element is less than 10 wt% then such types of steels are called medium carbon low alloy steels.

En8, En24, En26 and En41b are medium carbon low alloy steels and frequently used to make studs, bolts, rollers gears, axles, die holders, clutch plate, crankshaft and other machinery parts. Such steels are economical cheep & industrially viable because these have high tensile strength, high toughness and good machineability [101]. In the present competitive scenario, continuous improvement in material performance is an urgent need and the aforesaid alloys with present properties do not full-fill our requirements satisfactorily. In order to increase the surface micro-hardness and to improve the wear resistance of these low alloy steels, surface treatment is essentially needed.

Plasma nitriding is the most promising technique for the purpose of surface modification. This technique have many attractive properties such as, controlled process, single-step operation, excellent dimensional stability of components and also the fact that it is an environment-friendly technique [102]. Various studies on low alloy steels with plasma nitriding process are available in the literature [53, 102-104]. Mahboubi et al. [103] studied the duplex treatment (plasma nitriding and post oxidation) on plain carbon steel. Sirin et al. [53] studied the effect of process time on diffusion depth and surface micro-hardness on AISI 4340 steel. Corengia et al. [104] reported the micro-structural and topographical studies on AISI 4140 steel. Sun et al. [57] developed a mathematical model for the diffusion of nitrogen to simulate with the plasma nitriding process in low alloy steels. Results of such studies reveal that the plasma nitriding process parameters put great impact on surface properties of such low alloy steels.

Many industries required large diffusion depth to forge the material with hot-forging process, casting of material and for metallurgical applications. Therefore, in this chapter plasma nitriding process have been performed on En8, En24, En26 and En41b medium carbon low alloy steels for longer process time (10 h to 50 h) and obtained results have been reported. The details of the selected low alloy steel samples and obtained results are described in the subsequent sections. The details of the chemical composition and sample preparation are described in section 4.2. The results obtained from the various characterization techniques and results obtained from theoretical relation are explained section 4.3. The section 4.3.1 describes the results obtained from optical microscope and X-ray diffraction analysis. The detailed diffusion mechanism, linearly fitted equations with diffusion depth and polynomial fitting of micro-hardness with diffusion depth is discussed in section 4.3.2. The role of the alloying elements present in the low alloy steels during plasma nitriding process and calculated value of diffusion coefficient of nitrogen for all the selected steels are explained in section 4.3.3. Overall conclusions of the study are given in section 4.4.

4.2 Details of chemical composition and sample preparation

Samples used for assessment in this study are commercially available medium carbon low ally steel of En8, En24, En26 and En41b. The chemical compositions of these standard steels are given in the Table 4.1.

Table 4.1: Chemical compositions of selected low alloy steels.

Steel grade	**C**	**Mn**	**P**	**S**	**Si**	**Cr**	**Ni**	**Mo**	**Al**	**Fe**
En8	0.4	0.8	0.015	0.015	0.25					98.52
En24	0.4	0.6			0.3	1.2	1.5	0.25		95.75
En26	0.4	0.6			0.3	0.75	2.5	0.55		94.90
En41b	0.4	0.5			0.25	1.6		0.2	1.2	95.85

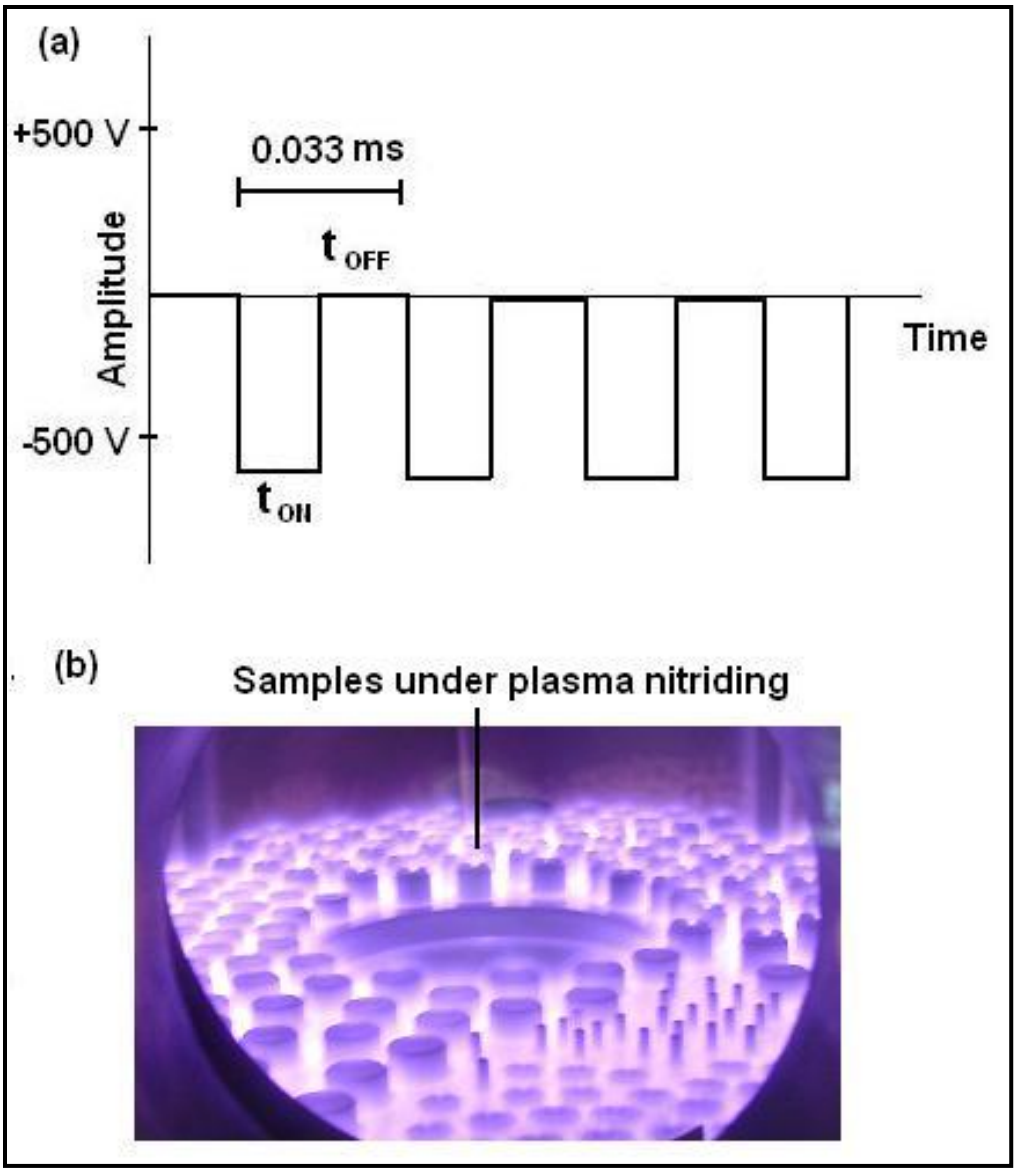

Figure 4.1: (a) Schematic representation of applied waveform, (b) Low alloy steel samples under plasma nitriding process.

Circular disc-shaped samples were prepared with 1.5 cm diameter and 2 cm thickness. Samples are polished with SiC emery papers of 240, 320, 400, 600, 800 grit size followed by diamond paste of 1 μm grain size and alumina paste of 0·05 μm grain size. After polishing, the prepared samples are washed with acetone for removal of dust/oil contamination from the surface and finally dried. After sufficient cleaning of the samples we have performed the plasma nitriding process. The typical plasma nitriding process parameters are given in the Table 4.2.

Table 4.2: Plasma nitriding process parameters.

Process Temperature (°C)	Gas Pressure (mbar)	Gas ratio H_2:N_2 %	Process Time (hours)	Applied Voltage (volts)
540	3	80 : 20	10 – 50	530 – 535

A schematic representation of the applied pulsed DC voltage waveform is shown in Figure 4.1 (a), and an image of low alloy steel samples under plasma nitriding process is shown in Figure 4.1 (b).

4.3 Results and Discussion

Under the defined operating parameters (refer Table 4.2), plasma nitriding process have been carried out for different process time on low alloy steel samples of varying alloying elements. The effect of plasma nitriding process time and effect of alloying elements on various surface properties of treated samples have been studied. Results are discussed below.

4.3.1 Microstructure and X-ray Diffraction Analysis

The microstructures of plasma nitrided samples obtained from optical microscope at two different process times 10 h and 50 h are shown in Figure 4.2. It is observed that there are substantial changes in the microstructures of plasma nitrided samples. These changes might have occurred due to the diffusion of nitrogen in the lattice structure in all the selected steels. A uniform ~6-8 µm thick compound zone in 10 h plasma treated samples has been observed. No significant increment is observed in the thickness of the compound zone with longer process time (50 h).

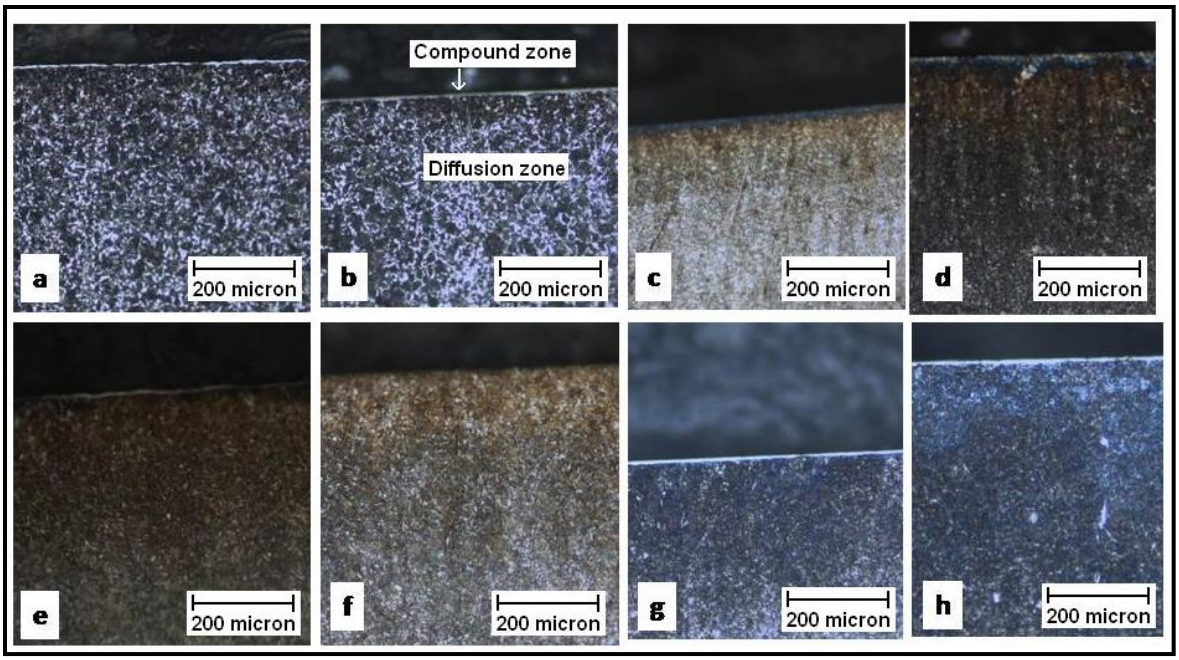

Figure 4.2: Microstructures of plasma nitrided samples (a) En8, 10hours, (b) En8, 50hours, (c) En24, 10hours, (d) En24, 50hours, (e) En26, 10hours, (f) En26, 50hours, (g) En41b, 10hours, (h) En41b, 50hours.

Corengia et al. [104] reported that most of the changes in compound zone thickness are observed within few hours of process initiation. A parabolic variation of compound zone thickness with process time was also observed. Below the compound zone, the microstructure of diffusion zone ranging up to few hundred microns was observed. The length of the diffusion zone is found to increase with process time in all the selected steels. For example, in En41b steel the diffusion zone extends from ~320 µm to ~620 µm as the process time is increased from 10h to 50h. The similar trends of variation in diffusion zone have also been reported by Sirin et al. [53] and Corengia et al. [104].

The results of X-ray diffraction analysis of selected steel samples for 10 h and 50 h treatment times are presented in Figure 4.3, 4.4, 4.5 and 4.6. XRD analysis shows the existence of γ-Fe_4N, and ε-$Fe_{2\text{-}3}N$ peak in all plasma treated samples at the surface.

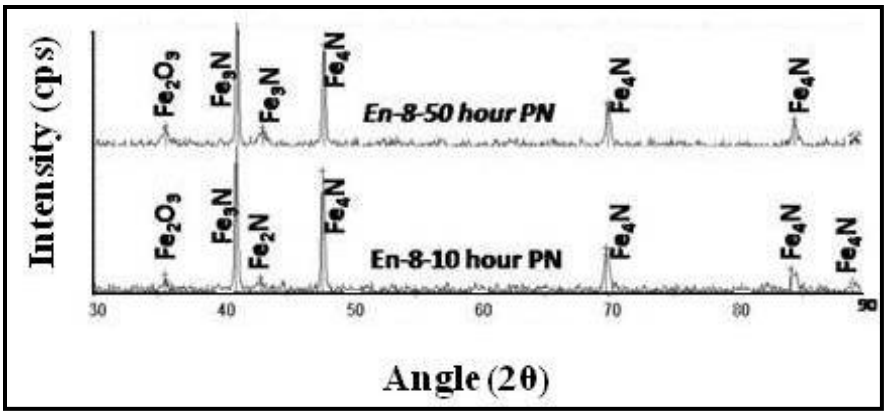

Figure 4.3: X-ray diffraction patterns of En8 steel samples for 10hours and 50hours.

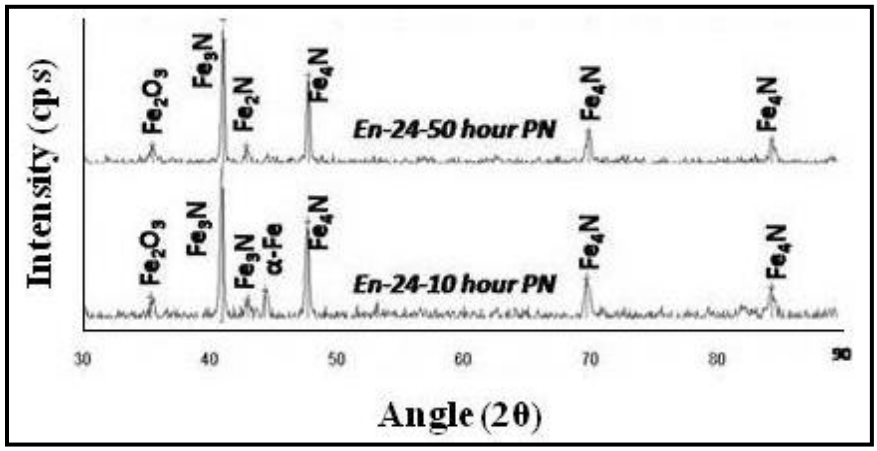

Figure 4.4: X-ray diffraction patterns of En24 steel samples for 10hours and 50hours.

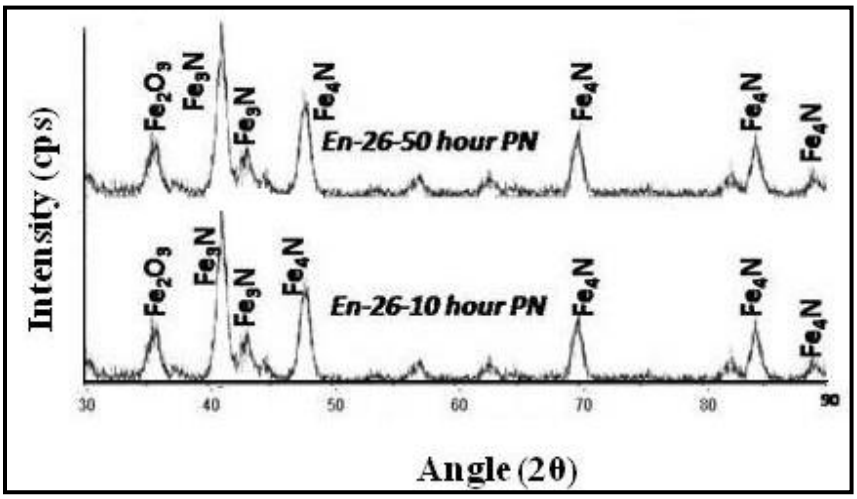

Figure 4.5: X-ray diffraction patterns of En26 steel samples for 10hours and 50hours.

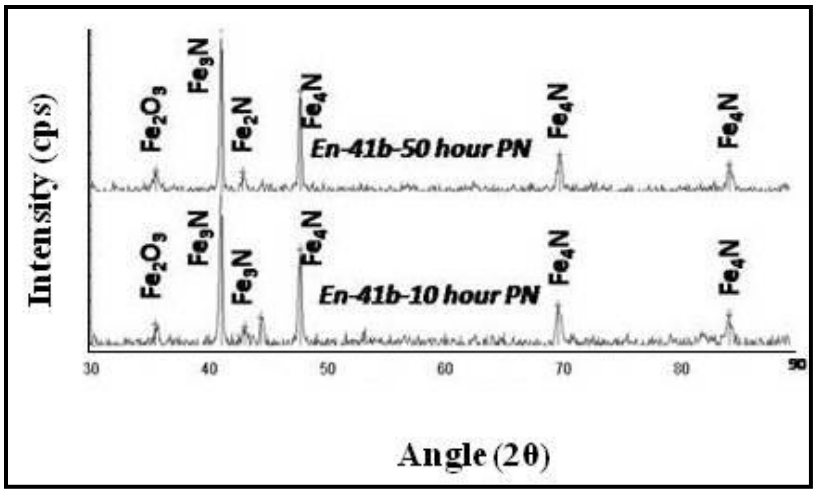

Figure 4.6: X-ray diffraction patterns of En41b steel samples for 10hours and 50hours.

The γ-Fe_4N peak is found dominant in all the plasma nitrided samples due the compound layer formation on the surface [53]. The obtained diffraction pattern indicates that the austenite (γ-Fe_4N) peak displaced slightly towards the lower 2θ angle. It might have been observed because of the austenite lattice expansion by introducing the nitrogen into the solid solution of steel during plasma nitriding. The similar results were observed by Somers et al. [105] for the plasma nitriding of different grades of steel. A hematite (Fe_2O_3) peak in all the plasma nitrided samples was also observed. This peak might be observed because of oxide formation during the cooling process after plasma nitriding. Mahboubi et al. [103] observed the similar hematite peak during the post oxidation process of plasma nitrided samples.

Further the XRD data was used for the calculation of size of grains formed on the surface of plasma nitrided samples from well known Scherer's relation (4.1) [97].

$$d = \frac{K\lambda}{\beta \cos\theta} \qquad (4.1)$$

here, *d* is the grain size, *K* is the shape factor which is generally taken as 0.9 for granular shape, λ is the wavelength of X-ray radiation, β is full width half maxima (FWHM) of the observed peak (in radian) and θ is the diffraction angle (in degree). For example, for En41b steel, typical value of K = 0.9, λ = 1.54Å, β = 0.6153 radian and θ = 42.2^0, the calculated d is ~33.93 nm. For the different values of β and θ corresponding to the

different peaks in XRD pattern, grain size varies in the range ~33.93 – 57.80 nm for 10 h process time while it varies ~34 – 63 nm for 50 h process time. The typical morphological image that exhibits the grain formation after plasma nitriding in selected steel treated for 10 h and 50 h are shown in Figure 4.7.

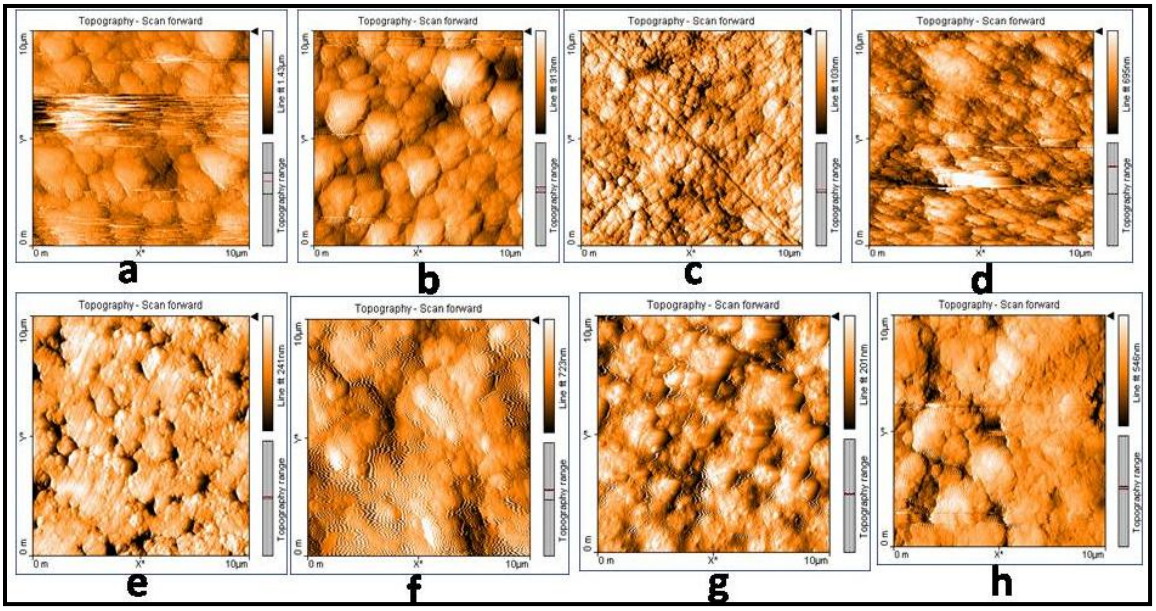

Figure 4.7: Morphological Images of plasma nitrided samples (a) En8, 10hours, (b) En8, 50hours, (c) En24, 10hours, (d) En24, 50hours, (e) En26, 10hours, (f) En26, 50hours, (g) En41b, 10hours, (h) En41b, 50hours.

This image has been captured by Nano-hardness measuring instrument. The typical average grain size as measured from this morphological image is ~100 nm. It is in close agreement with the grain size calculated using equation (1) with XRD data. The bigger size grains are observed to form at 50 h process time as compared to 10 h process time. It is seen that as plasma nitriding process starts, the formation of small nuclei of iron-nitride as well as other nitrides starts on the surface. With the increase of process time, the amount of various nitrides formed during plasma nitriding also increases. It leads to increased grain size due to nucleation growth process [106].

4.3.2 Diffusion Kinetics

The results of XRD analysis reveal the formation of iron-nitrides (γ-Fe_4N and ε-$Fe_{2\text{-}3}N$) on the surface during plasma nitriding process. In addition to iron-nitrides various other

types of nitrides such as; chromium-nitride, aluminium-nitride etc are also formed. These additional nitrides are generally difficult to identify in XRD analysis due to their smaller size and density as compared to iron-nitrides. However, the formation of these nitrides plays a significant role to alter the surface properties e.g. wear, hardness etc. of treated alloy steel. These nitrides are further diffused in the interior of the sample through a thermo-chemical diffusion process.

Diffusion mechanism is relevant to understand plasma nitriding process in a better way. Generally, various types of diffusion processes such as vacancy diffusion, interstitial diffusion and self diffusion etc. are possible in solids. In most of the metal alloys, interstitial diffusion dominates and occurs rapidly than other diffusion processes. In the general sense, diffusion is a time dependent process that is initiated if there exists a finite concentration gradient. For steady-state conditions (time independent concentration), the diffusion process is expressed by Fick's first law [99] as given below,

$$J = -D \frac{dC}{dx} \qquad (4.2)$$

Where, *J* is the diffusion flux, *D* is the diffusion coefficient (expressed in m^2/s) and *C* is the concentration of diffusing species.

For non-steady state conditions, diffusion is dependent on position and time. For such cases (e.g. plasma nitriding, carburizing etc.), the diffusion equation is modified and given by Fick's second law [99] as given below,

$$\frac{\partial C}{\partial t} = D \frac{\partial^2 C}{\partial x^2} \qquad (4.3)$$

Under fixed surface boundary conditions, equation (4.3) can be simplified as,

$$x = Constant \sqrt{(D.t)} \qquad (4.4)$$

In plasma nitriding process results x is referred as diffusion depth (X), t is referred as process time and D is referred as diffusion coefficient of nitrogen (D_N) in to selected low alloy steel samples. For simplification constant is taken as unity [107]. Therefore, equation (4.4) can be rewritten in our case in the following form

$$X = \sqrt{(D_N . t)} \quad (4.5)$$

To verify this theoretical relation (Eq. 4.5) in our experiments, we have plotted experimentally measured diffusion depth (X) in our low-alloy steel samples as a function of square root of process time ($t^{1/2}$) at constant process temperature ~540 ^{0}C.

Further a linear fitting is done for all the experimental variations as shown in Figure 4.8. The linear fitted equations for each steel that describe the layer growth kinetics are written as,

$$X = -3.44 + 49.03t^{1/2} \quad \text{(for En8 steel)} \quad (4.6.a)$$

$$X = 146.55 + 49.03t^{1/2} \quad \text{(for En24 steel)} \quad (4.6.b)$$

$$X = 205.07 + 50.59t^{1/2} \quad \text{(for En26 steel)} \quad (4.6.c)$$

$$X = 89.65 + 78.99t^{1/2} \quad \text{(for En41b steel)} \quad (4.6.d)$$

The obtained linear equations (Eq. (4.6.a)-(4.6.d)) represent that experimental observations follow the theoretical predictions of diffusion process as given by equation 4.5. It is clear from Figure 4.8 that the diffusion depth increases linearly with square root of process time. It is important to note from Equation (4.6.a) - (4.6.d) that, a finite value of diffusion layer thickness exists even the process time is taken as zero in plasma nitriding process. Similar argument on the layer growth has been proposed by Sun [108] in the case of the plasma carburizing process of austenitic stainless steel. As a suitable clarification of this analysis, it is observed that there is a broad range of plasma nitriding process temperature generally varies from 450 ^{0}C to 580 ^{0}C. Hence the plasma nitriding process and formation of a thin nitrided layer is initiated much earlier before our plasma nitriding process temperature (~ 540 ^{0}C) is reached. It indicates that the heating cycle of the material during plasma nitriding process also plays a significant role in the growth of nitrided layer on steel surface.

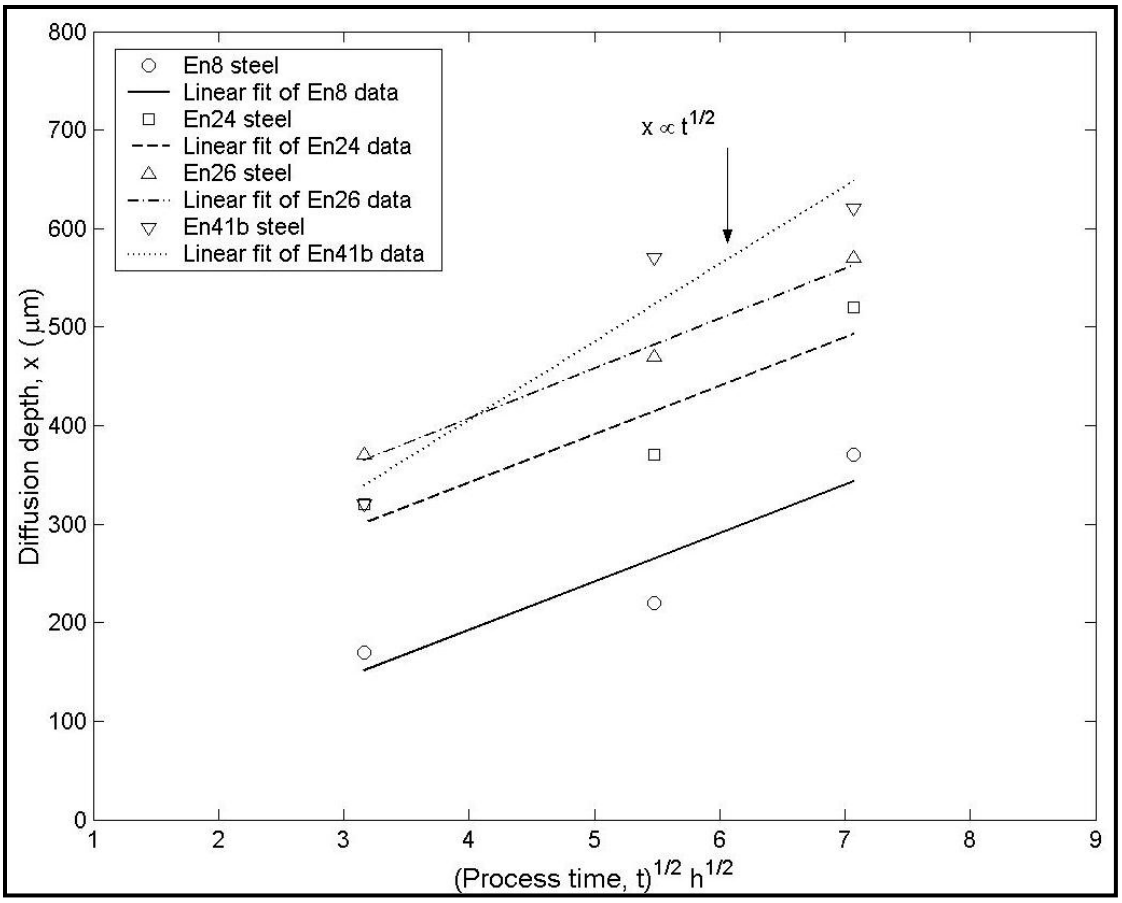

Figure 4.8: Linear fitting of experimental variations.

Figure 4.9 shows the variation of measured micro-hardness with diffusion depth of plasma nitrided samples at different process time. The micro-hardness is observed to decrease from surface to core region in all the steel samples. It might be observed because of decrease in diffused nitrogen concentration towards the core region. Similar micro-hardness profile has also been observed by Sirin et al. [53] and Scheuer et al. [109].

A polynomial fit of the micro-hardness profiles with diffusion depth of plasma nitrided steel (En 41b) has been obtained which is shown in Figure 4.10. It shows that the micro-hardness in core region is inversely proportional to square of diffusion depth (surface to core) and hence follows a power law $H \propto X^{-2}$. It is also observed that the micro-hardness in the core region beyond the diffusion depth remains nearly unchanged in all the treated samples.

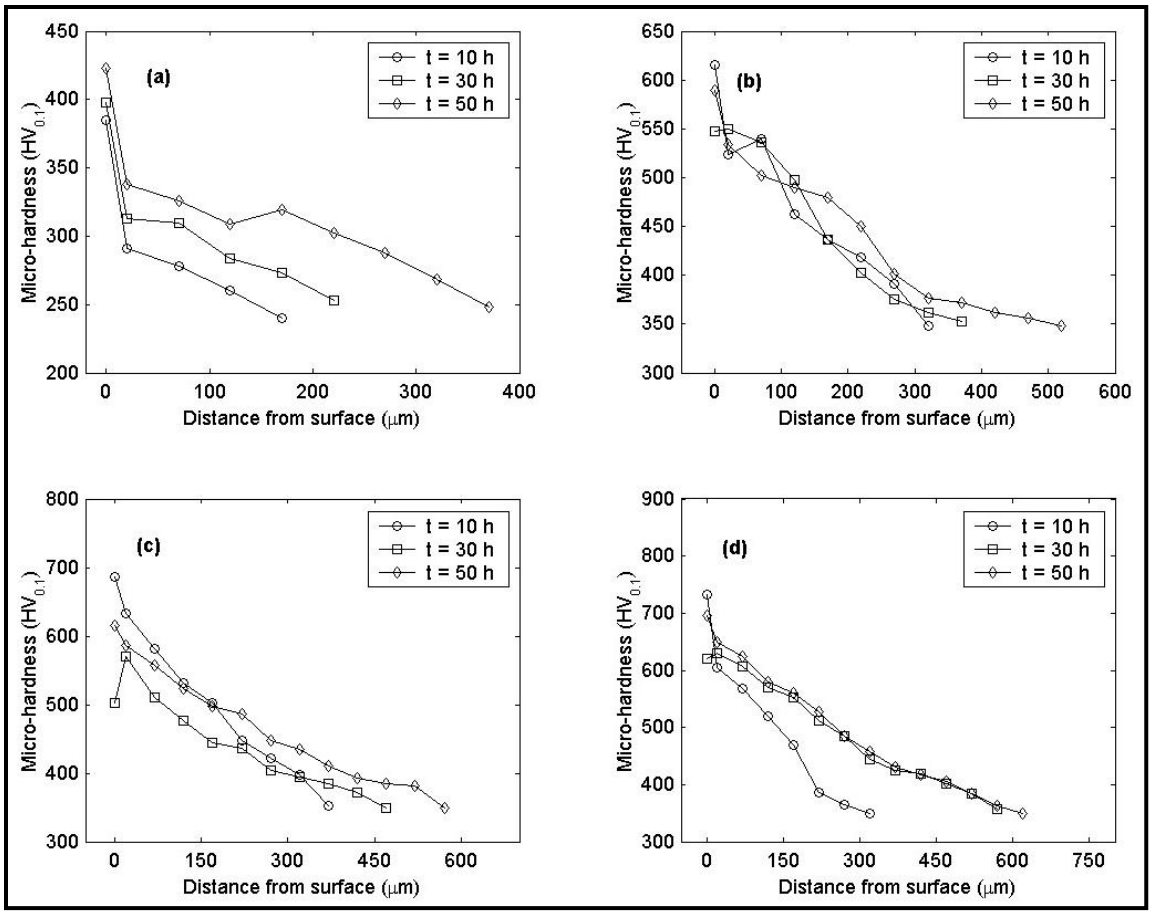

Figure 4.9: Variation of measured micro-hardness with diffusion depth (a) En8, (b) En24, (c) En26, (d) En41b.

In figure 4.11 surface micro-hardness profile of plasma nitrided samples with variation of process times (10 h to 50 h) has been plotted for further discussion. Initially, the surface micro-hardness increases drastically with process time in all the steel samples. However, for longer process time (more than 10 h) the surface micro-hardness seems to be decreased. Similar trend of surface micro-hardness with process time was observed by Sirin et al. [53] for medium carbon AISI 4340 low alloy steel. This reduced surface micro-hardness behavior is basically related to the formation of larger size nitride precipitates. These nitrides are less effective to increase surface micro-hardness as compared to smaller size nitrides [53, 110]. The lower surface micro-hardness at initial process time may be attributed to low nitrogen uptake leading to low nitride precipitate density.

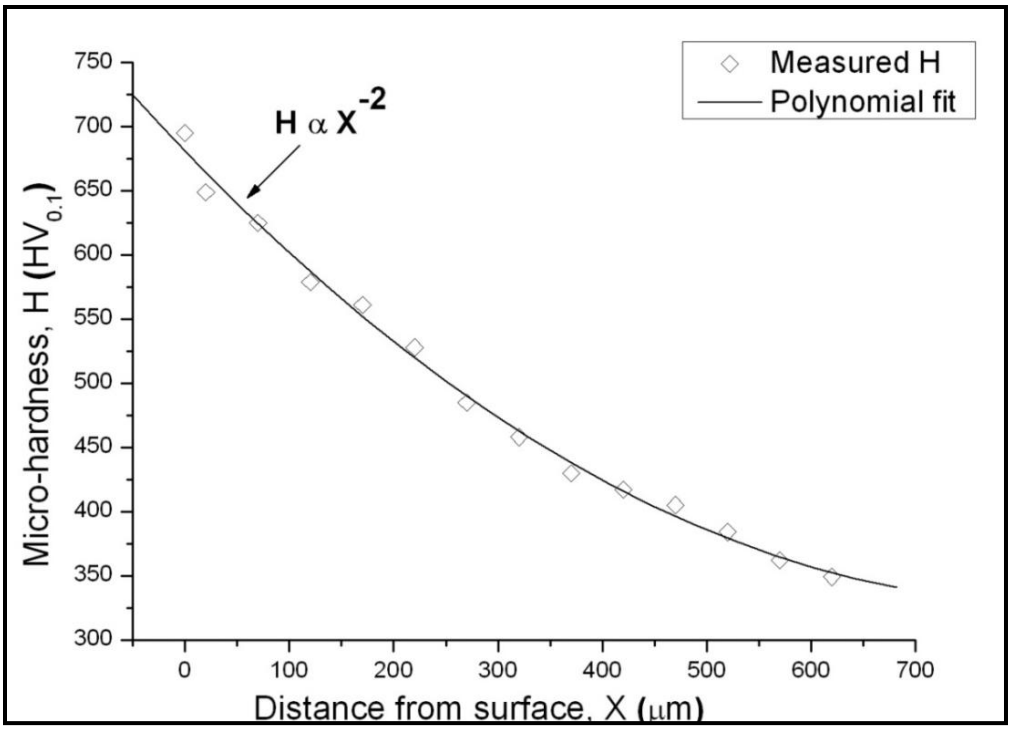

Figure 4.10: Polynomial fit of the micro-hardness profiles with diffusion depth.

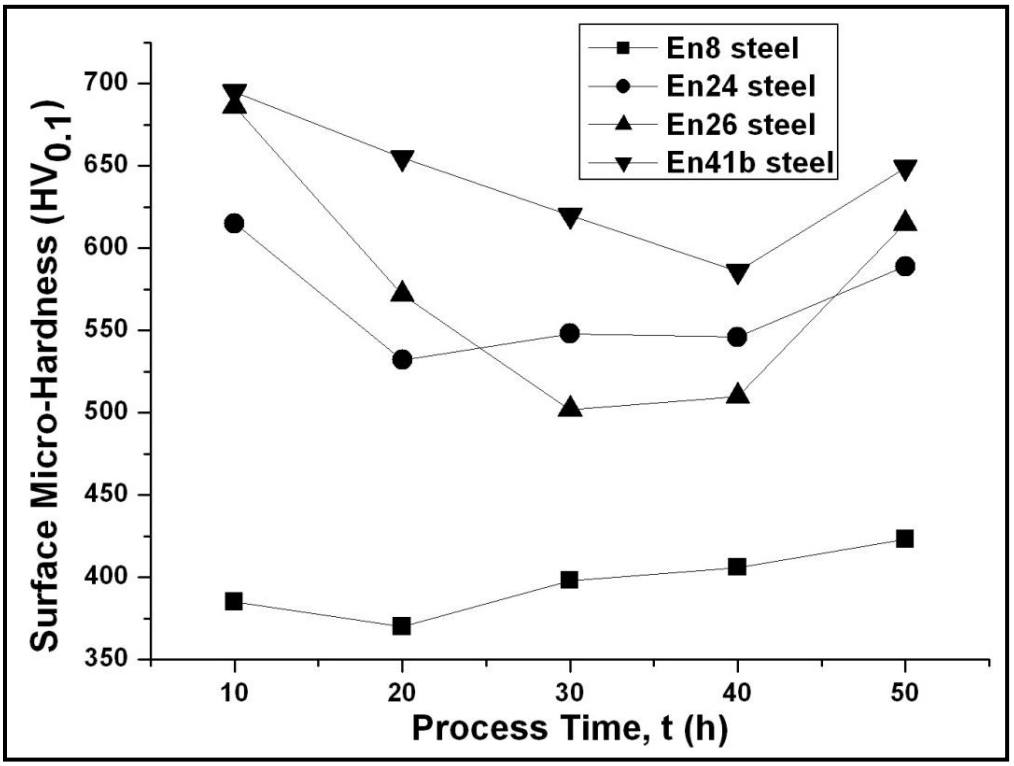

Figure 4.11: Surface micro-hardness profiles of plasma nitrided samples with variation of process time.

Karamiş et al. [110] also argued that at higher temperature and longer process time, growth in precipitate density and tempering of the steel become important that leads the lower surface micro-hardness. The grain growth of the nitride with process time is also confirmed by grain size calculation from our earlier XRD analysis.

4.3.3 Role of Alloying Elements on Surface Hardness and Diffusion Depth

Referring Table 4.1, it is clear that the selected low-alloy steels are differentiated by the concentration of present alloying elements. Based on the investigations and analysis after plasma nitriding treatment, the role of such alloying elements to modify the surface as well as diffusion properties of steel samples has been analyzed. Diffusion coefficient of nitrogen (D_N) in the selected low-alloy steels using Equation (4.5) at different process time has been calculated. For En41b steel, at typical t = 10 h, X = 320 µm the D_N is 2.8×10^{-12} m^2/s. The value of D_N (averaged over process time) is plotted for each low alloy steels as shown in Figure 4.12.

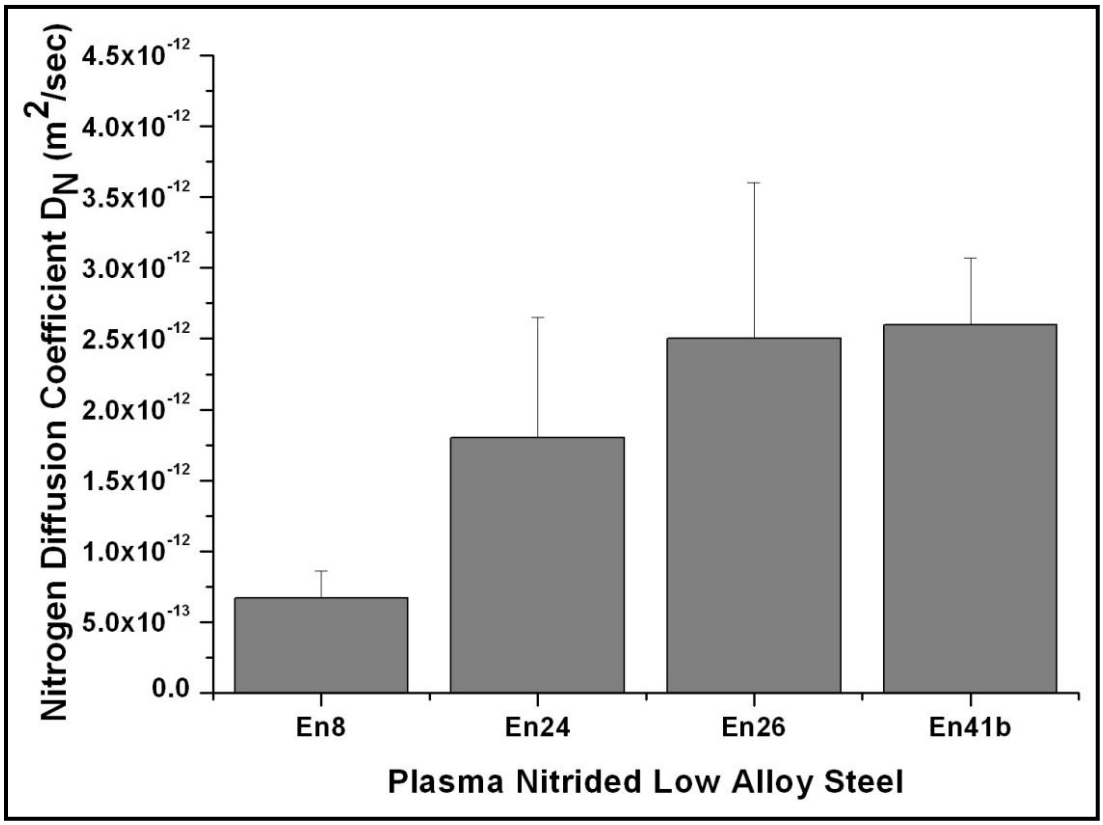

Figure 4.12: Values of nitrogen diffusion coefficient (D_N) for each low alloy steel.

It is observed that D_N value differs for these steels. It indicates that the type (Cr, Al, Mo etc) & content (%) of alloying elements (refer Table 4.1) present in the selected steels plays a significant role in plasma nitriding. As a result of nitrogen interaction with the surface of low alloy steel, various nitrides are formed. Apart from the dominant iron nitrides, few additional nitrides (CrN, AlN etc) are also formed due to strong affinity of nitrogen with the alloying elements. The chemical reactions of chromium and aluminum with nitrogen for the formation of nitrides during plasma nitriding process are given below,

$$2\,Cr + N_2 = 2\,CrN \quad (4.7)$$

$$2\,Al + N_2 = 2\,AlN \quad (4.8)$$

These nitrides are mainly responsible to alter the surface properties such as surface micro-hardness and diffusion depth. It is observed that the En-41b steel which is having these nitride forming elements (Cr, Al) with maximum concentration is able to attain maximum surface micro-hardness (~732 HV) and diffusion depth (620 µm) as compared to other steels. Egawa et al. [55] have also suggested that the presence of strong nitride forming elements enhances the nitrogen diffusion depth in austenitic stainless steels. Goune et al. [56] also observed the role of chromium for increasing the diffusion of nitrogen in the bulk of the material. Sun et al. [57] explored, in detail, the presence of chromium percentage to limit the diffusion depth in plasma nitriding. This study importantly reveals that the diffusion depth of nitrogen increases with increase in Cr% till 1% while it decreases with more enhanced Cr %. It has been reported that with increased in Cr content above 1%, more CrN will be formed at surface that consumes a lot of diffusing nitrogen. It increases the surface micro-hardness however, the hardness at interior of the sample decreases due to reduction in diffusing nitrogen. This effect is primarily seen in the case of stainless steels with large Cr content [108].

In this study it was not able to observe effect of more Cr content on low-alloy steels with ~ 1% Cr. It is to be noted that in these steels, both En24 & En26 steels are having Cr element. En24 is having relatively more Cr% (1.2%) than En26 steel (0.75%) but the

surface micro-hardness and diffusion depth are found more in En26 steel. The reason behind this observation might be the presence of other alloying elements (Mo, Ni) with more % in En26 steel. Hence these alloying elements (Mo, Ni) also help to diffuse the nitrogen deep inside the material. Sun et al. [57, 108] observed the similar results on the layer growth kinetics in different austenitic stainless steels and reported that molybdenum (Mo) can improve the diffusion kinetics at lower temperature. En8 steel which is not having these nitride forming elements exhibits minimum surface micro-hardness ~385 HV and diffusion depth (370 μm).

However, very little information is available to justify or predict the role of a particular alloying element quantitatively, Sun et al. [108] have given the model calculations of free energy (ΔG) of few alloying elements (Cr, V, Al, Ti) with 1% concentration in the nitriding interaction processes. It is seen that the free energy that may be a measure of nitrogen diffusion, for such alloys follows the sequence ($\Delta G_{Cr} > \Delta G_V > \Delta G_{Al} > \Delta G_{Ti}$). It may be a reason of more diffusion depth and hardness for our En41b steel as compared to other steels. It is concluded that the presence of nitride forming elements (type, number and concentration) put a significant impact in plasma nitriding process to alter the surface properties. Specific steels samples should be selected with optimized characteristics of alloying elements before performing a plasma nitriding treatment needed for a particular application.

4.4 Conclusion

In this study, four different low alloy steels (En-8, En-24, En-26, and En-41b) have been plasma nitrided and analyzed for effect of process time and alloying elements. Following conclusions are obtained,

(1) The microstructure of treated samples shows the presence of a thin compound zone (~6–8 μm) on the surface. A substantially thick diffusion zone (few hundred μm) is also observed as a result of diffusion of nitrogen inside the steel. Diffusion zone thickness varies in different low alloy steels.

(2) Measured XRD patterns reveal the presence of (γ-Fe_4N, and ε-$Fe_{2-3}N$) nitride peaks in all plasma treated samples. It is also observed that grain-size at the

nitrided layer increases with process time. The calculated grain-size (~63 nm) was close to the value (~100 nm) measured from morphological image.

(3) The experimentally measured diffusion depth (X) increases linearly with square root of process time ($t^{1/2}$) following Fick's second law of diffusion. The growth of diffused layer starts during heating process before the desired process temperature is achieved.

(4) The surface micro-hardness is initially observed to increase with process time however it decreases with longer process time. The variation of micro-hardness (H) with diffusion distance from the surface (diffusion depth, *X*) follows a power law $H \propto X^{-2}$. For longer process time diffusion depth and micro-hardness exhibit inverse trend. For longer process time, growth in precipitate density and tempering of the steel become important that reduce the surface micro-hardness.

(5) Alloying elements and their concentrations present in the steel sample are observed to play a significant role in achieving desired surface micro-hardness and diffusion depth. It is important to state that, if the steel has strong nitride forming elements (Cr, Al, Mo etc.) under low concentration (~ 1-2%), the diffusion depth and hardness will be more.